IEEE Access
Multidisciplinary | Rapid Review | Open Access Journal

Received October 31, 2021, accepted November 7, 2021, date of publication November 15, 2021,
date of current version November 24, 2021.

Digital Object Identifier 10.1109/ACCESS.2021.3128168

Achievable Rate Enhancement Based on Multi-Packet Indexing in Packet-Level Index Modulation

RIKU YAMABE[1], MIKIHIKO NISHIARA[1], (Member, IEEE), OSAMU TAKYU[1], (Member, IEEE), AND KOICHI ADACHI[2], (Senior Member, IEEE)

[1]Department of Electrical and Computer Engineering, Shinshu University, Matsumoto, Nagano 380-8553, Japan
[2]Advanced Wireless and Communication Research Center, The University of Electro-Communications, Chofu, Tokyo 182-8585, Japan

Corresponding author: Osamu Takyu (takyu@shinshu-u.ac.jp)

This work was supported in part by the Ministry of Internal Affairs and Communications in Japan through the project name Strategic Information and Communications Research and Development Promotion Programme (SCOPE) under Grant JP205004001, and in part by the Japan Society for the Promotion of Science (JSPS) KAKENHI under Grant JP 18K04131.

ABSTRACT The low-power wide area (LPWA) limits the access duration defined by the duty cycle (DC) to avoid mutual interference among the systems. Packet-level index modulation (PLIM) uses the frequency channel and the transmission timing of a packet as an information-bearing index. LPWA with PLIM can increase the number of information bits without changing the wireless communication standards despite adherence to the DC limits. However, there is still a gap between the achievable rate and the channel capacity. Multi-packet indexing determines an information-bearing index based on multiple packets. Thus, it can exploit the channel more efficiently, which results in an increased achievable rate. This study derives a mathematical formula for the achievable rate of PLIM with multi-packet indexing and clarifies the rate enhancement brought by it.

INDEX TERMS Low power wide area, packet-level index modulation, multi-packet indexing.

I. INTRODUCTION

A low-power wide area (LPWA) comprises long-range and low-power wireless networks in the unlicensed and sub-GHz bands. Because the LPWA can send a packet of small data to the data center (fusion center) with high efficiency, it is suitable for wireless sensor networks (WSNs) [1]. In the sub-GHz bands, multiple wireless systems, such as LoRa [2], Sigfox [3], and WiSUN [4], share common frequency bands [5]. To avoid mutual interferences, the LPWA imposes limitations on the data transmission duration, which is defined by the duty cycle (DC) [6]. The DC limits the throughput and access opportunities to the data center (fusion center), and it is thus a bottleneck for the LPWA.

Index modulation (IM) has recently gained significant attention [7]. In this scheme, the baseband signal modulated by phase-shift keying and quadrature amplitude modulation uses the channel number, timing of the signal appearance, and transmit antenna number as the indexes for information encoding. The data can be transmitted not only by baseband modulation, but also by IM. Therefore, additional information can be transmitted through the revised channel model so that the achievable rate, which is the information amount sent to the receiver without error, is enlarged. IM based on the transmit antenna selection is referred to as spatial modulation [7]; it enlarges the achievable rate without incrementing the bandwidth, thereby achieving a high-frequency usage efficiency. If the IM is applied to orthogonal frequency division multiplexing (OFDM), the subcarrier selection pattern can be used as an information-bearing index [8].

A WSN operating based on IM is a powerful wireless communication scheme for the enhancement of the achievable rate. However, the sensor requires multiple antennas for spatial modulation, and the simplicity and low-cost construction of the sensor are not attained. The physical modulation format is changed in the subcarrier selection based on OFDM and the selection of the modulation format. Therefore, the design and implementation of an integrated circuit for the physical modulation of IM are significantly expensive. In addition, the practical realization of IM is time-consuming because the wireless communication standard should be revised.

The associate editor coordinating the review of this manuscript and approving it for publication was Prakasam Periasamy.

Packet-level index modulation (PLIM) transmits additional information bits by selecting a combination of the frequency channel and the access timing of a packet as an information-bearing index [9]. PLIM uses the time-domain sparsity due to the DC [6], i.e., it splits the transmission period (i.e., a frame) into multiple time slots to define a timing index. PLIM utilizes the channel more refinedly by sending additional information without changing the physical layer packet format. Therefore, PLIM does not require a change in the wireless communication standards; hence, the existing wireless communication module can be used for PLIM. Since the original study assumes that only one packet is transmitted per frame [9], i.e., we call it single-packet indexing; it cannot fully utilize the available channel. Thus, there is still a gap between the achievable rate of PLIM with single-packet indexing and the capacity of a multi-frame channel. In [10], we proposed PLIM with multi-packet indexing, in which multiple packets define an index. Letting multiple packets define an index produces more available indexes than single-packet indexing, especially with low DC. Suppose the DC limits the number of packets a transmitter can transmit per specific time duration. PLIM with single-packet indexing cannot efficiently utilize the capacity of a channel consisting of multiple frames. On the other hand, PLIM with multi-packet indexing efficiently utilizes the available capacity of a multi-frame channel and thus enhances the achievable rate.

The capability of PLIM with multi-packet indexing has not been clarified in terms of the achievable rate in [10]. Therefore, this paper aims to analyze the achievable rate of the PLIM with the multi-packet indexing and its upper limit is positioned as the important initial study. So far, the achievable rate increase brought by PLIM with multi-packet indexing and its limit have not been clarified yet.

The contributions of this paper are as follows:

- The authors derived the achievable rate of PLIM subject to the packet erasure channel model in [10] but the explanation of derivation is not easily understandable. This paper shows the detailed derivation of it for deeper understanding.
- We proposed multi-packet indexing to improve the achievable rate of PLIM [10]. This paper further improves the achievable rate via information-theoretical analysis of the multi-packet indexing.
- The authors derived the upper limit of the achievable rate per frame for PLIM with multi-packet indexing without packet erasure in [10]. This paper derived it under the condition that packet erasure may occur. Consequently, we recognize the gap of the achievable rate between the multi-packet indexing and the upper limit. This can be used as a design metric.

The remainder of this paper is organized as follows. Relevant prior studies are summarized in Section 2. The channel model of the PLIM is explained in Section 3. This is followed by the derivation of the mathematical formula for the achievable rate of the PLIM in Section 4. The limit of the achievable rate is presented in Section 5. In Section 6, the numerical results are demonstrated for the evaluation of the achievable rate of the PLIM. Finally, the conclusions are presented in Section 7.

II. RELATED WORKS

The derivation and enlarging scheme of the achievable rate or the channel capacity for IM have been considered previously. The channel capacity of the IM was derived in the frequency domain and its advantages compared with the space-time block code [11]. The bounds for the capacity of the IM in the spatial domain have also been derived [12], [13]. The channel capacity of an IM based on the spatial, polarized, and frequency domains was derived based on closed-form expressions using second- and fourth-order approximations [14]. The channel capacity for the time-indexed and media-based modulation has also been derived [15]. In this derivation, the media-based modulation used the channel gain to convey additional information [16]. In PLIM, it is necessary to consider the information conveyed by both a packet and an index to derive the achievable rate. To the authors' best knowledge, the upper limit of the achievable rate of the PLIM has not been described yet.

Various types of IM have been proposed thus far. In a frequency-diverse array with increasing signal frequencies for each element, the increment of frequency is used as the index for information-bearing [17]. Spatial modulation was implemented by an aperture antenna composed of metamaterials [18]. The impact of intercarrier interference through the high-speed, time-selective channel on the IM was clarified, and the optimized construction of the precoder and post-processing for maximizing the channel capacity was derived [19]. IM-based polarized antenna selection in a polarized antenna bank was also proposed [20]. Additionally, compressed sensing was introduced to the IM [21], [22] and then applied to millimeter-wave communications [23].

Maximum likelihood detection was used to minimize the average error rate for the detection of the IM [24]. In the IM of the subcarrier selection type, a subcarrier group was constructed to enhance frequency diversity without the channel state information [25]. The IM-based spread spectrum modulation, orthogonal modulation, and spatial modulation were considered in a multi-input multi-output system, and the error rate was derived based on a theoretical analysis [26]. The total construction of the IM and channel coding has also been considered; for example, spatial modulation based on antenna selection and trellis coding has been proposed [27]. The selection of both the subcarrier and signal constellation for IM has been reported [28], [29]. The optimized construction of IM with energy detection was considered for the asynchronous receiver [30]. The combination of various schemes of wireless communications and IM has been considered, such as chaos modulation [31] and multiple access schemes [32].

PLIM constructs the indexes on a packet basis [9]. In PLIM, the parallel data transmission through the data

packet and information-bearing index becomes available. Multi-packet indexing increases the number of indexes by jointly considering multiple packets. Thus, it is necessary to understand the reasonable number of packets used for multi-packet indexing subject to memory size limitations and the delay time of data transmission. Herein, the upper limit of the achievable rate of PLIM with multi-packet indexing is derived. This derivation clarifies the reasonable number of packets for multi-packet indexing.

III. CHANNEL MODEL OF PLIM

Figure 1 presents an overview of PLIM and the format of the packet. There are K number of channels. The packet is composed of L bits. The slot is identified as the time index, and its length is determined by the duration of transmission of a single packet.

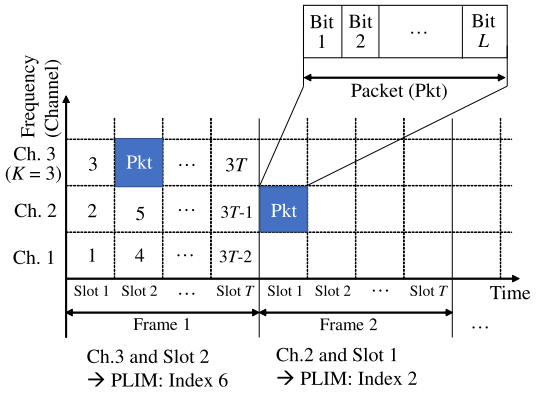

FIGURE 1. Packet-level index modulation (PLIM).

This paper does not assume any specific type of information for data to be transmitted by packet and index, which can be environmental monitoring information etc. A transmitter splits the information sequence into two sequences. The transmitter modulates the first sequence into a data packet the same way as the conventional LPWA systems. The transmitter encodes the second information sequence into an information-bearing index, i.e., the combination of frequency channel and time slot. Then, the transmitter transmits a data packet on the selected frequency channel and time slot.

A frame is composed of T slots. In our model, the transmission of packets obeys the DC of the LPWA. Namely, N packets are transmitted within NT slots in $(N = 1, 2, \ldots)$. According to the new regulations of LPWA, the sensor can transmit multiple packets by accessing multiple channels, despite the single packet access per frame being maintained. This study does not consider the enhancement of multi-packet access per frame via multiple channel access.

This study aims to derive the achievable rate limitation and determine a reasonable number of packets for the enlargement of the achievable rate of PLIM with multi-packet indexing. The achievable rate of PLIM with multi-packet indexing is determined by the packet delivery rate, or equivalently, by the packet erasure probability. The performance of PLIM is determined by the following two parts: the information sequence transmitted by the LPWA modulation scheme within a packet, and the information sequence transmitted by an index. Given that PLIM with multi-packet indexing does not modify any of the LPWA modulation schemes, the performance of the former is the same as the conventional LPWA. Thus, the error rate performance [33] and the outage probability of wireless LPWA sensor networks [34] assume that practical channel models, such as multipath fading, can be applied directly. The performance of the latter part is an essential factor for achievable rate enhanced by PLIM. The rationale behind the use of the packet erasure channel in this study is as follows. As long as the receiver demodulates a packet without error, it can retrieve an index. Thus, it can demodulate the information sequence transmitted by the index. If a packet is received with an error, we consider the packet and its corresponding index lost. We can assume the discrete packet erasure channel model as the channel of PLIM. Specifically, the erasure probability is a function of the bit error probability derived based on the continuous-time channel model. The error rate performance of LPWA under the continuous-time channel model has been derived [33]. Thus, the erasure channel model can evaluate the performance of the information sequence transmitted by an index. Therefore, this study adopts the packet erasure channel as the channel model.

The transmitted packets are erased with a certain probability, which is referred to as the erasure probability, defined as ε. If the packet is erased, the receiver does not detect the data bits of the packet or the PLIM data, that is, the index for the channel and slot. This study considers the access channel from a single transmitter (sensor) to the receiver (fusion center). The packet reception error arises in practical wireless communication systems due to the channel gain drop or interference. This system can be modeled as a packet erasure channel with different erasure probabilities.

Figure 2 presents an example of the PLIM without and with multi-packet indexing, wherein the number of frames is set to $N = 2$. Since the transmitter transmits one packet only during each frame when multi-packet indexing is not applied, the number of indexes becomes $(KT)^N$. On the other hand, when multi-packet indexing is applied, the transmitter transmits more than one packet within N frames. Thus, the number of indexes can be increased. We derive the number of indexes and achievable rate expression for PLIM with multi-packet indexing. Note that we do not consider the order of packets. In addition, we assume that each sensor is equipped with a single radio transceiver that cannot access two or more channels in a slot. Therefore, the number of patterns for selecting the slots is $\binom{NT}{N}$. In each slot, the sensor accesses one channel selected from K channels; therefore, the number of access channel patterns within N frames is K^N, and the number of indexes is $K^N \binom{NT}{N}$. Figure 3 presents an example of the set indexes, where the indexes are normalized by the number of frames, N, and their bit domain can be obtained by the binary logarithm. The number of channels, K, and the number of

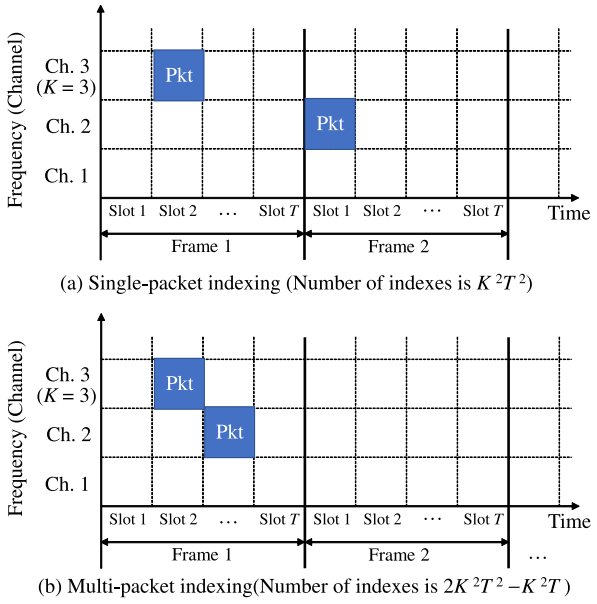

FIGURE 2. Examples single- and multi-packet indexing when $N = 2$.

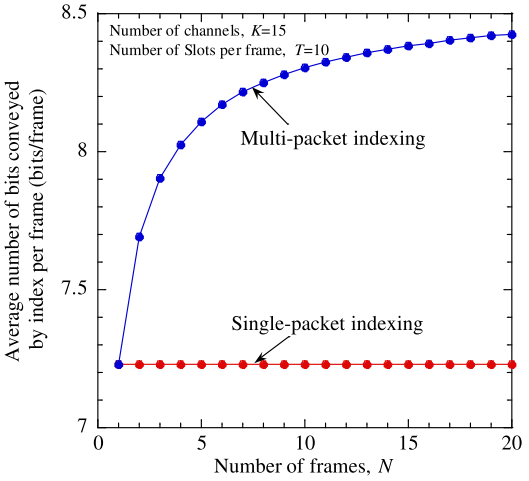

FIGURE 3. Average number of indexes per frame vs. number of frames N ($K = 15, T = 10$).

slots per frame, T, are 15 and 10, respectively. As N becomes larger, the number of indexes with multi-packet indexing is larger than that with single-packet indexing. Therefore, an increment in the achievable rate by multi-packet indexing is expected.

Figure 4 shows the architectures of a transmitter and receiver in the PLIM with multi-packet indexing. Their architectures are the same as those for PLIM [9], except for the memories. The transmitter accumulates the sensing data for the formulation of a multi-packet index. The receiver accumulates the received multiple packets to achieve multi-packet indexing demodulation.

This study assumes that the overhead of the packet header is ignored. The achievable rate [35] is derived in the following section. In this study, the radix of the log function is 2.

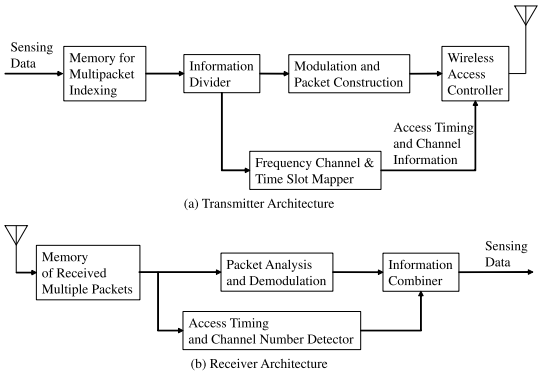

FIGURE 4. Architecture of packet-level index modulation (PLIM) with multi-packet indexing.

IV. DERIVATION OF ACHIEVABLE RATE

A. CASE WITHOUT MULTI-PACKET INDEXING

We begin with a special case in which we transmit one packet within a frame ($N = 1$). In this case, the number of indexes is KT. In addition, a packet obtains a value among 2^L patterns. Therefore, the size of the input alphabet of the channel is $KT \times 2^L$. We define a symbol as a pair of a packet and its index. In Figure 5, $S_1, S_2, \ldots$ and S_Q indicate the label of the input symbol, where $Q = KT \times 2^L$. $*$ denotes the "erasure symbol," which means that the receiver receives no packets. We can obtain the achievable rate as the channel capacity of an erasure channel since the channel model here is an erasure channel with an input alphabet of size Q and an output alphabet of size $Q+1$. From the well-known result for erasure channels, the achievable rate of a packet per frame, $C_{1,\varepsilon}$, is

$$C_{1,\varepsilon} = (1 - \varepsilon)(L + \log KT). \tag{1}$$

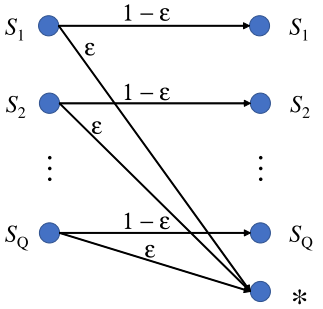

FIGURE 5. Transition model of a packet erasure channel.

If the PLIM is not used, the achievable rate cannot exceed $(1 - \varepsilon)L$ (bits/frame). Therefore, $(1 - \varepsilon) \log KT$ is the basic enhancement achieved by PLIM.

B. CASE WITH MULTI-PACKET INDEXING

We derive the achievable rate of the PLIM with multi-packet indexing. In this case, we have to extend the notion of "symbol." We define a symbol as an N-tuple of pairs of packets and its index. In other words, a single symbol denotes N packets and its indexes transmitted in N frames. Therefore, the size of the input alphabet is $K^N \binom{NT}{N} 2^{NL}$. Note that erasure of a

packet does not mean erasure of a symbol because the decoder can restore a partial information from the rest of received packets. The output alphabet has many incomplete symbols in addition to the symbols in the input alphabet. This channel model is not an erasure channel and we cannot employ the result of erasure channels. Let $C_{N,\varepsilon}$ denote the achievable rate when N packets are transmitted within N frames with an erasure probability ε for $N \geq 1$. The following theorem is a fundamental result of this study.

Theorem 1:

$$C_{N,\varepsilon} = \log\left(K^N \binom{NT}{N} (2^L)^N\right) - \sum_{i=0}^{N} \binom{N}{i} \varepsilon^i (1-\varepsilon)^{N-i} \log\left(K^i \binom{NT-(N-i)}{i} (2^L)^i\right). \tag{2}$$

Proof 1: The achievable rate is obtained by deriving the capacity of the channel model. When a symbol is input into the channel, that is, when N packets are transmitted, the sample space for the channel output consists of 2^N points owing to erasing the packets. We partition this sample space in $N+1$ events in accordance with the number of erased packets. The probability that specified i packets are erased is $\varepsilon^i(1-\varepsilon)^{(N-i)}$ for $i = 0, 1, \ldots, N$. Let X and Y denote random variables for the input and output of the channel, respectively. The conditional entropy $H(Y|X=x)$ is given as

$$H(Y|X=x) = -\sum_{i=0}^{N} \binom{N}{i} \varepsilon^i (1-\varepsilon)^{N-i} \log \varepsilon^i (1-\varepsilon)^{N-i} \tag{3}$$

for every channel input x. Because this does not depend on x, we have

$$\begin{aligned} H(Y|X) &= \sum_x \Pr\{X=x\} H(Y|X=x) \\ &= -\sum_{i=0}^{N} \binom{N}{i} \varepsilon^i (1-\varepsilon)^{N-i} \log \varepsilon^i (1-\varepsilon)^{N-i}. \end{aligned} \tag{4}$$

Following the conditional entropy, we also address $H(Y)$. As a function of X, $H(Y)$ is maximized by the uniform distribution of X, as shown in Appendix 1. Under the condition that X is uniformly distributed, we consider the probability of a received symbol with specific i packets erased, $P_e(i)$. The number of input symbols, each of which provides the received symbol by i packet erasures, is $K^i\binom{NT-(N-i)}{i}(2^L)^i$. Therefore,

$$P_e(i) = \frac{K^i \binom{NT-(N-i)}{i} (2^L)^i}{K^N \binom{NT}{N} (2^L)^N} \varepsilon^i (1-\varepsilon)^{N-i}. \tag{5}$$

Moreover, the number of received symbols with i erased packets is $K^{N-i}\binom{NT}{\text{N-i}}(2^L)^{N-i}$. Therefore, the entropy of the received symbol Y, $H(Y)$, is derived as follows:

$$\begin{aligned} H(Y) &= -\sum_{i=0}^{N} K^{N-i} \binom{NT}{\text{N-i}} (2^L)^{N-i} P_e(i) \log P_e(i) \\ &= -\sum_{i=0}^{N} \binom{N}{i} \varepsilon^i (1-\varepsilon)^{N-i} \log P_e(i). \end{aligned} \tag{6}$$

Therefore, the achievable rate is given as follows:

$$\begin{aligned} C_{N,\varepsilon} &= I(X;Y) \\ &= H(Y) - H(Y|X) \\ &= -\sum_{i=0}^{N} \binom{N}{i} \varepsilon^i (1-\varepsilon)^{N-i} \log \frac{P_e(i)}{\varepsilon^i (1-\varepsilon)^{N-i}} \\ &= \log\left(K^N \binom{NT}{N} (2^L)^N\right) \\ &\quad - \sum_{i=0}^{N} \binom{N}{i} \varepsilon^i (1-\varepsilon)^{N-i} \\ &\quad \times \log\left(K^i \binom{NT-(N-i)}{i} (2^L)^i\right). \end{aligned} \tag{7}$$

Note, this is a generalization of Eq. (1).

V. UPPER LIMIT OF ACHIEVABLE RATE

We derived the achievable rate $C_{N,\varepsilon}$, which is the maximal information within N frames through the channel. We consider the asymptotic behavior of $C_{N,\varepsilon}/N$. Because this value monotonically increases with respect to N, the limit that N goes to ∞ yields the upper limit.

A. CASE WITHOUT PACKET ERASURE

We first consider the special case wherein there is no packet erasure ($\varepsilon = 0$). This case can serve as the basis for the general case. In addition, we consider that the derivation of the achievable rate without erasure helps the reader understand that with erasure.

Theorem 2:

$$\lim_{N\to\infty} \frac{1}{N} C_{N,0} = \log K(2^L) + T\log T - (T-1)\log(T-1). \tag{8}$$

Proof 2: Based on Theorem 1, we have

$$\begin{aligned} \frac{1}{N} \times C_{N,0} &= \frac{1}{N} \times \log \binom{NT}{N} K^N (2^L)^N \\ &= \log K(2^L) + \frac{1}{N} \log \frac{NT!}{N!(NT-N)!} \\ &= \log K(2^L) + \frac{1}{N} \log NT! - \frac{1}{N} \log N! \\ &\quad - \frac{1}{N} \log (NT-N)!. \end{aligned} \tag{9}$$

In accordance with Stirling's formula[1], the approximation of the achievable rate is given as follows,

$$\begin{aligned} &\frac{1}{N} \times C_{N,0} \\ &\simeq \log K(2^L) + \frac{1}{N} \log \sqrt{2\pi NT} \left(\frac{NT}{e}\right)^{NT} \\ &\quad - \frac{1}{N} \log \sqrt{2\pi N} \left(\frac{N}{e}\right)^{N} \end{aligned}$$

[1] $N! \simeq \sqrt{2\pi N}\left(\frac{N}{e}\right)^N$, where $f(N) \simeq g(N)$ means $f(N)/g(N) \to 1$ as $N \to \infty$.

$$
\begin{aligned}
&- \frac{1}{N}\log\sqrt{2\pi(NT-N)}\left(\frac{NT-N}{e}\right)^{NT-N} \\
&= \log K(2^L) + T\log T - (T-1)\log(T-1) \\
&\quad + \frac{1}{N}(\log\sqrt{2\pi NT} - \log\sqrt{2\pi N} - \log\sqrt{2\pi(NT-N)}).
\end{aligned} \tag{10}
$$

In this equation, the terms related to N become

$$
\lim_{N\to\infty}\frac{1}{N}(\log\sqrt{2\pi NT} - \log\sqrt{2\pi N} - \log\sqrt{2\pi(NT-N)}) = 0. \tag{11}
$$

Therefore, the upper limit of the achievable rate per frame without packet erasure is derived as follows,

$$
\lim_{N\to\infty}\frac{1}{N}C_{N,0} = \log K(2^L) + T\log T - (T-1)\log(T-1). \tag{12}
$$

B. CASE WITH PACKET ERASURE

We consider herein the general case in which packet erasure may occur ($\varepsilon \geq 0$). In the proof of this case, we employed the law of large numbers for a binominal distribution. This effect is attributed to packet erasure.

Theorem 3:

$$
\begin{aligned}
\lim_{N\to\infty}\frac{C_{N,\varepsilon}}{N} \simeq{}& (1-\varepsilon)\log K(2^L) + T\log T + \varepsilon\log\varepsilon \\
&- (T-1+\varepsilon)\log(T-1+\varepsilon).
\end{aligned} \tag{13}
$$

Proof 3: Equation (2) can be modified as follows:

$$
\begin{aligned}
C_{N,\varepsilon} ={}& \log\left(K^N\binom{NT}{N}(2^L)^N\right) \\
&- \sum_{i=0}^{N}\binom{N}{N-i}\varepsilon^i(1-\varepsilon)^{N-i}\log\left(K^i(2^L)^i\right) \\
&- \sum_{i=0}^{N}\binom{N}{N-i}\varepsilon^i(1-\varepsilon)^{N-i}\log\binom{NT-(N-i)}{i} \\
={}& \log\left(K^N\binom{NT}{N}(2^L)^N\right) \\
&- \log\left(K(2^L)\right)\sum_{i=0}^{N}\binom{N}{N-i}\varepsilon^i(1-\varepsilon)^{N-i}\times i \\
&- \sum_{i=0}^{N}\binom{N}{N-i}\varepsilon^i(1-\varepsilon)^{N-i}\{\log(NT-(N-i))! \\
&- \log(NT-N)! - \log(i)!\}.
\end{aligned} \tag{14}
$$

The logarithmic version of Stirling's formula[2] is applied to the factorial components of the third term. The approximation of the achievable rate is derived as follows:

$$
\begin{aligned}
C_{N,\varepsilon} \simeq{}& \log\left(K^N\binom{NT}{N}(2^L)^N\right) \\
&- \sum_{i=0}^{N}\binom{N}{N-i}\varepsilon^i(1-\varepsilon)^{N-i}\log\left(K^i(2^L)^i\right) \\
&- \sum_{i=0}^{N}\binom{N}{N-i}\varepsilon^i(1-\varepsilon)^{N-i} \\
&\times\{(NT-(N-i)\log(NT-(N-i)) \\
&- (NT-N)\log(NT-N) - (i)\log(i)\}.
\end{aligned} \tag{15}
$$

[2] $\log N! \simeq (N\log N) - N$.

TABLE 1. Parameter set for PLIM.

Data bits per packet L	Time Length of a slot (ms)	Number of slots per frame T	Time length of frame (s)
10	4.5	96	4.4
40	18.3	24	4.4

Therefore, the achievable rate per frame is derived as

$$
\begin{aligned}
\frac{C_{N,\varepsilon}}{N} \simeq{}& \frac{1}{N}\times\log\left(K^N\binom{NT}{N}(2^L)^N\right) \\
&- \frac{1}{N}\times\log\left(K(2^L)\right)\sum_{i=0}^{N}\binom{N}{N-i}\varepsilon^i(1-\varepsilon)^{N-i}i \\
&- \sum_{i=0}^{N}\binom{N}{N-i}\varepsilon^i(1-\varepsilon)^{N-i} \\
&\times\left\{\left(T-\left(1-\frac{i}{N}\right)\right)\log(NT-(N-i)) \right. \\
&\left. - (T-1)\log(NT-N) - \frac{i}{N}\log(i)\right\}.
\end{aligned} \tag{16}
$$

We now introduce the random variable J with the binomial distribution with parameters N and ε. Eq. (16) can then be rewritten as an expression using J, that is,

$$
\begin{aligned}
\frac{C_{N,\varepsilon}}{N} \simeq{}& \frac{1}{N}\times\log\left(K^N\binom{NT}{N}(2^L)^N\right) \\
&- \frac{1}{N}\times\log\left(K(2^L)\right)E[J] \\
&- E\left[\left(T-\left(1-\frac{J}{N}\right)\right)\log(N(T-(1-\frac{J}{N}))) \right. \\
&\left. - (T-1)\log(N(T-1)) - \frac{J}{N}\log(N\times\frac{J}{N})\right],
\end{aligned} \tag{17}
$$

where $E[\cdot]$ denotes the expectation operation. From the law of large numbers [36], we have $J/N \to \varepsilon$ as $N \to \infty$. As a result,

$$
\begin{aligned}
\lim_{N\to\infty}\frac{C_{N,\varepsilon}}{N} ={}& \log K(2^L) + T\log T - (T-1)\log(T-1) \\
&- \varepsilon\log K(2^L) - (T-1+\varepsilon)\log(T-1+\varepsilon) \\
&+ (T-1)\log(T-1) + \varepsilon\log\varepsilon \\
={}& (1-\varepsilon)\log K(2^L) + T\log T + \varepsilon\log\varepsilon \\
&- (T-1+\varepsilon)\log(T-1+\varepsilon).
\end{aligned} \tag{18}
$$

A detailed explanation of $\frac{J}{N} \to \varepsilon$ is provided in Appendix 2.

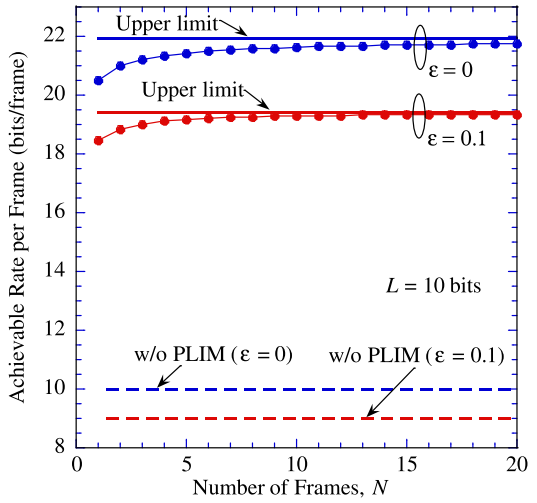

FIGURE 6. Achievable rate per frame as a function of number of frames N ($L = 10$ [bits]).

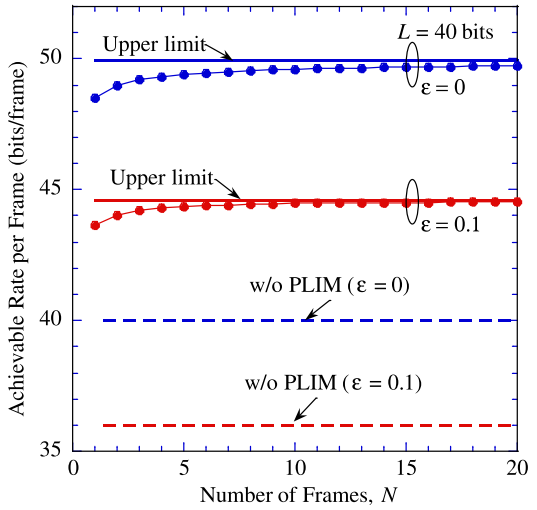

FIGURE 7. Achievable rate per frame as a function of number of frames N ($L = 40$ [bits].

VI. NUMERICAL RESULTS

This section presents the numerical results of the achievable rate of the PLIM. Table 1 lists the relationships among the data bits per packet L, time length of a slot, number of slots per frame T, and time length of the frame. This study assumes that the time length of the frame is constant.

Figures 6 and 7 demonstrate the performance between the number of frames and the achievable rate per frame when the data sizes of packet L are 10 and 40, respectively. The horizontal axes of these figures indicate the number of frames N for multi-packet indexing. The number of channels K is 15. In the figures, the solid lines with a circle plot indicate the exact achievable rate of LoRa employing PLIM with multi-packet indexing, which is obtained by Eq. (2). When $N = 1$, the solid lines with a circle plot represent the achievable rate of LoRa employing PLIM with single-packet indexing [9]. The solid lines present the upper limit of the achievable rate obtained by Eqs. (8) and (13). For comparison, the achievable rate of LoRa without PLIM is also plotted as dashed lines.

In both figures, the achievable rate per frame increases as a function of the number of frames. We confirmed the increment of the achievable rate according to multi-packet indexing. In $L = 10$, the differences in the achievable rate between $N = 1$ and the upper limit are 1.5 bits/frame in $\varepsilon = 0$ and 1.0 bits/frame in $\varepsilon = 0.1$, respectively. In $L = 40$, these differences are the same as those for $L = 10$. These can be considered as a limitation of the increment of the achievable rate owing to multi-packet indexing. As the erasure probability increases, the degradation of the increment of the achievable rate owing to multi-packet indexing is confirmed.

As the number of frames N increases, the achievable rate of PLIM approaches the upper limit irrespective of the erasure probability ε, due to the increased number of indexes in multi-packet indexing. For example, when $N = 20$, the achievable rate is almost equal to the upper limit for $\varepsilon = 0.1$, despite the fact that the difference is 0.2 bits/frame for $\varepsilon = 0$. Although an additional achievable rate increase is expected, the achievable rate of PLIM with multi-packet indexing does not increase owing to the fact that the packet is erased beyond $N = 20$. As a result, the achievable rate of PLIM with multi-packet indexing almost saturates at $N = 20$.

The difference between the upper limit of the achievable rate of PLIM with multi-packet indexing and that without PLIM can be explained as follows. When $\varepsilon = 0$, the difference between the upper limit of the achievable rate of PLIM with multi-packet indexing, and that without PLIM is 12 bits/frame and 10 bits/frame for $L = 10$ and $L = 40$, respectively. Table 1 shows that the time length of a slot becomes larger at larger L values. Therefore, the number of slots within a fixed-length frame becomes smaller, resulting in a decrease in the number of indexes for PLIM. As a result, the difference between the upper limit of the achievable rate of PLIM with multi-packet indexing and that without PLIM decreases as L becomes larger.

As the number of frames is greater than five, the difference in the achievable rate from the upper limit is smaller than 5 bits/frame. The delay of the packet arrival increases as a function of the number of frames for multi-packet indexing, and the memory size for recording multiple data packets in the sensor also increases. By considering a smaller delay of packet arrival and a smaller memory size of the sensor, and by obtaining a large increment of achievable rate owing to multi-packet indexing, the five frames are reasonable at the parameters assumed in this study.

VII. CONCLUSION

This study derived mathematical formulas for the achievable rate of packet-level index modulation (PLIM) with multi-packet indexing and its upper limit by considering packet erasure probability. The numerical evaluation based on the derived formulas clarified the achievable rate enhancement by multi-packet indexing. The comparison between the upper limit and the achievable rate of PLIM with multi-packet

indexing is useful for the parameter setting of PLIM and multi-packet indexing. Furthermore, the impact of the packet erasure on the PLIM with multi-packet indexing was clarified. The derived expression can be a rough indication of the practical throughput of PLIM with multi-packet indexing. The timely practical implementation of PLIM to wireless sensor networks is expected because PLIM requires no change in the standardization and no additional hardware implementation.

Clarifying the gap between the practical throughput and the derived achievable rate is left as an important future work. In this study, we assumed the operation of one node. Random access from multiple nodes caused packet collision, which has an impact on the achievable rate. The derivation of the achievable rate in multi nodes environment remains an important topic for future study.

APPENDIX 1

To demonstrate that the uniform input distribution maximizes the mutual information of our channel, we introduce the concept of the "symmetry" of a channel according to [37]. Our channel has $Q = K^N \binom{NT}{N} \cdot 2^{NL}$ input symbols. Let R denote the number of output symbols, where $R = \sum_{n=0}^{N} K^n \binom{nT}{n} \cdot 2^{nL}$. The input and output alphabets are denoted by $\mathcal{X} = \{S_1, \ldots, S_Q\}$ and $\mathcal{Y} = \{S_1, \ldots, S_R\}$, respectively. A channel is described by the conditional probabilities $W(y|x) = \Pr\{Y = y|X = x\}$, $x \in \mathcal{X}$, and $y \in \mathcal{Y}$.

Definition 1: A channel W is said to be *uniformly dispersive* if, for any two inputs $x, x' \in \mathcal{X}$, $(W(S_1|x), \ldots, W(S_R|x))$ is one of the permutation outcomes of $(W(S_1|x'), \ldots, W(S_R|x'))$.

Definition 2: A channel W is said to be *uniformly focusing* if $\sum_{i=1}^{Q} W(y|S_i)$ is a constant that does not depend on the output symbol y.

Definition 3: A channel is said to be *strongly symmetric* if it is both uniformly dispersive and uniformly focusing.

Definition 4: A channel is said to be *symmetric* if, for some value of N, it can be decomposed in $N + 1$ strongly symmetric channels. Precisely,

$$W(y|x) = q_i W_i(y|x), \quad \text{if } y \in \mathcal{Y}_i \tag{19}$$

with appropriate selection probabilities $q_0, q_1, \ldots, q_N$, where W_i, $i = 0, \ldots, N$ are strongly symmetric channels with the output alphabet $\mathcal{Y}_i$, and $\{\mathcal{Y}_i\}_{i=0}^{N}$ is a partition of $\mathcal{Y}$.

Our channel is symmetric. To justify this, partition $\mathcal{Y}$ into $\mathcal{Y}_i$, $i = 0, \ldots, N$ according to the number i of the erased packets. The subset $\mathcal{Y}_i$ has $K^{N-i}\binom{(N-i)T}{N-i} \cdot 2^{(N-i)L}$ symbols. The selection probability is $q_i = \binom{N}{i}\varepsilon^i(1-\varepsilon)^{N-i}$.

The following theorem [37] yields the desired conclusion.

Theorem 4: For a symmetric channel, the uniform input distribution achieves the capacity.

APPENDIX 2

We demonstrate that $J/N \to \varepsilon$ as $N \to \infty$, according to the law of large numbers [36]. N and ε denote the number of transmitted packets and the erasure probability of the packet, respectively. The random variable J denotes the number of erased packets. Let X_i be a binary random variable with a value of one if the ith packet is erased. Otherwise, its value is zero. Then, we have

$$J = \sum_{i=1}^{N} X_i. \tag{20}$$

According to the law of large numbers, $\frac{J}{N}$ is reformed as follows:

$$\frac{J}{N} = \frac{1}{N}\sum_{i=1}^{N} X_i \tag{21}$$

$$\to E[X_1] \tag{22}$$

$$= \varepsilon. \tag{23}$$

REFERENCES

[1] U. Raza, P. Kulkarni, and M. Sooriyabandara, "Low power wide area networks: An overview," *IEEE Commun. Surveys Tuts.*, vol. 19, no. 2, pp. 855–873, 2nd Quart., 2017.

[2] M. Gohar, S. H. Ahmed, M. Khan, N. Guizani, A. Ahmad, and A. U. Rahman, "A big data analytics architecture for the internet of small things," *IEEE Commun. Mag.*, vol. 56, no. 2, pp. 128–133, Feb. 2018.

[3] W. Yang, M. Wang, J. Zhang, J. Zou, M. Hua, T. Xia, and X. You, "Narrowband wireless access for low-power massive Internet of Things: A bandwidth perspective," *IEEE Wireless Commun.*, vol. 24, no. 3, pp. 138–145, Jun. 2017.

[4] C.-S. Sum, H. Harada, F. Kojima, Z. Lan, and R. Funada, "Smart utility networks in TV white space," *IEEE Commun. Mag.*, vol. 49, no. 7, pp. 132–139, Jul. 2011.

[5] G. Hattab and D. Cabric, "Spectrum sharing protocols based on ultra-narrowband communications for unlicensed massive IoT," in *Proc. IEEE Int. Symp. Dyn. Spectr. Access Netw. (DySPAN)*, Oct. 2018, pp. 1–10.

[6] R. M. Sandoval, A.-J. Garcia-Sanchez, J. Garcia-Haro, and T. M. Chen, "Optimal policy derivation for Transmission duty-cycle constrained LPWAN," *IEEE Internet Things J.*, vol. 5, no. 4, pp. 3114–3125, Aug. 2018.

[7] N. Ishikawa, S. Sugiura, and L. Hanzo, "50 years of permutation, spatial and index modulation: From classic RF to visible light communications and data storage," *IEEE Commun. Surveys Tuts.*, vol. 20, no. 3, pp. 1905–1938, 3rd Quart., 2018.

[8] N. Ishikawa, S. Sugiura, and L. Hanzo, "Subcarrier-index modulation aided OFDM–will it work?" *IEEE Access*, vol. 4, pp. 2580–2593, 2016.

[9] K. Adachi, K. Tsurumi, A. Kaburaki, O. Takyu, M. Ohta, and T. Fujii, "Packet-level index modulation for LoRaWAN," *IEEE Access*, vol. 9, pp. 12601–12610, 2021.

[10] R. Yamabe, M. Nishiara, and O. Takyu, "Channel capacity for a model of packet level index modulation in LPWA networks," in *Proc. 12th Int. Conf. Ubiquitous Future Netw. (ICUFN)*, Aug. 2021, pp. 339–344.

[11] Y. Yang and B. Jiao, "Information-guided channel-hopping for high data rate wireless communication," *IEEE Commun. Lett.*, vol. 12, no. 4, pp. 225–227, Apr. 2008.

[12] R. Rajashekar, K. V. S. Hari, and L. Hanzo, "Reduced-complexity ML detection and capacity-optimized training for spatial modulation systems," *IEEE Trans. Commun.*, vol. 62, no. 1, pp. 112–125, Jan. 2014.

[13] R. Zhang, L.-L. Yang, and L. Hanzo, "Error probability and capacity analysis of generalised pre-coding aided spatial modulation," *IEEE Trans. Wireless Commun.*, vol. 14, no. 1, pp. 364–375, Jan. 2015.

[14] P. Henarejos and A. I. Pérez-Neira, "Capacity analysis of index modulations over spatial, polarization, and frequency dimensions," *IEEE Trans. Commun.*, vol. 65, no. 12, pp. 5280–5292, Dec. 2017.

[15] B. Shamasundar, L. N. Theagarajan, and A. Chockalingam, "Capacity analysis of time-indexed media-based modulation," in *Proc. IEEE Wireless Commun. Netw. Conf. (WCNC)*, May 2020, pp. 1–6.

[16] A. K. Khandani, "Media-based modulation: A new approach to wireless transmission," in *Proc. IEEE Int. Symp. Inf. Theory*, Jul. 2013, pp. 3050–3054.

[17] S. Y. Nusenu, S. Huaizong, Y. Pan, and A. Basit, "Space-frequency increment index modulation approach for fifth generation and beyond wireless communication systems," *IEEE Trans. Veh. Technol.*, vol. 69, no. 6, pp. 6286–6298, Jun. 2020.
[18] J. A. Hodge, K. V. Mishra, and A. I. Zaghloul, "Reconfigurable metasurfaces for index modulation in 5G wireless communications," in *Proc. Int. Appl. Comput. Electromagn. Soc. Symp. (ACES)*, Apr. 2019, pp. 1–2.
[19] J. Zheng and R. Chen, "Linear processing for intercarrier interference in OFDM index modulation based on capacity maximization," *IEEE Signal Process. Lett.*, vol. 24, no. 5, pp. 683–687, May 2017.
[20] Z. Lai, J. Jiang, F. Zhu, and Y. Chen, "Impulse index modulation with polarized antenna bank," in *Proc. Inf. Commun. Technol. Conf. (ICTC)*, May 2020, pp. 222–225.
[21] S. Lu, I. A. Hemadeh, M. El-Hajjar, and L. Hanzo, "Compressed sensing-aided multi-dimensional index modulation," *IEEE Trans. Commun.*, vol. 67, no. 6, pp. 4074–4087, Jun. 2019.
[22] J. Choi, "Sparse index multiple access," in *Proc. IEEE Global Conf. Signal Inf. Process. (GlobalSIP)*, Dec. 2015, pp. 324–327.
[23] I. A. Hemadeh, S. Lu, M. El-Hajjar, and L. Hanzo, "Compressed sensing-aided index modulation improves space-time shift keying assisted millimeter-wave communications," *IEEE Access*, vol. 6, pp. 64742–64756, 2018.
[24] S. Lu, M. El-Hajjar, and L. Hanzo, "Two-dimensional index modulation for the large-scale multi-user MIMO uplink," *IEEE Trans. Veh. Technol.*, vol. 68, no. 8, pp. 7904–7918, Aug. 2019.
[25] M. Wen, X. Cheng, M. Ma, B. Jiao, and H. V. Poor, "On the achievable rate of OFDM with index modulation," *IEEE Trans. Signal Process.*, vol. 64, no. 8, pp. 1919–1932, Apr. 2016.
[26] E. Aydin, F. Cogen, and E. Basar, "Code-index modulation aided quadrature spatial modulation for high-rate MIMO systems," *IEEE Trans. Veh. Technol.*, vol. 68, no. 10, pp. 10257–10261, Oct. 2019.
[27] A. Vincent and B. K. Jeemon, "A bandwidth efficient coding technique for spatial modulation and its error performance," in *Proc. Int. Conf. Appl. Theor. Comput. Commun. Technol. (iCATccT)*, Oct. 2015, pp. 195–200.
[28] X. Yu and J. Pang, "Performance evaluation of OFDM index modulation with LDPC code," in *Proc. IEEE 31st Annu. Int. Symp. Pers., Indoor Mobile Radio Commun.*, Aug. 2020, pp. 1–5.
[29] C. An and H.-G. Ryu, "Dual-mode OFDM with coded direct index modulation for the spectrum efficiency improvement," in *Proc. Int. Conf. Comput. Netw. Commun. (CoCoNet)*, Aug. 2018, pp. 1–5.
[30] A. Fazeli and H. H. Nguyen, "Code design for non-coherent index modulation," *IEEE Commun. Lett.*, vol. 24, no. 3, pp. 477–481, Mar. 2020.
[31] W. Xu, Y. Tan, F. C. M. Lau, and G. Kolumbán, "Design and optimization of differential chaos shift keying scheme with code index modulation," *IEEE Trans. Commun.*, vol. 66, no. 5, pp. 1970–1980, May 2018.
[32] Y.-T. Lai, Y.-R. Ciou, and J.-M. Wu, "Index modulation multiple access," in *Proc. IEEE 29th Annu. Int. Symp. Pers., Indoor Mobile Radio Commun. (PIMRC)*, Sep. 2018, pp. 1–5.
[33] T. Elshabrawy and J. Robert, "Closed-form approximation of LoRa modulation BER performance," *IEEE Commun. Lett.*, vol. 22, no. 9, pp. 1778–1781, Sep. 2018.
[34] T. H. Nguyen, W.-S. Jung, L. T. Tu, T. Van Chien, D. Yoo, and S. Ro, "Performance analysis and optimization of the coverage probability in dual hop LoRa networks with different fading channels," *IEEE Access*, vol. 8, pp. 107087–107102, 2020.
[35] T. M. Cover and J. A. Thomas, *Elements of Information Theory*, 2nd ed. Hoboken, NJ, USA: Wiley, 2006.
[36] A. Papoulis and S. Pillai, *Probability, Random Variables, and Stochastic Processes*, 4th ed. New York, NY, USA: McGraw-Hill, 2002.
[37] J. L. Massey, "Applied digital information theory I. Lecture notes," Signal, Inf. Process. Lab., ETH Zürich, Switzerland, Tech. Rep., 1998. [Online]. Available: http://www.isiweb.ee.ethz.ch/archive/masseyscr/

RIKU YAMABE received the B.E. degree from the Department of Electrical and Electronic Engineering, Shinshu University, in 2021. His research interest includes wireless communication systems.

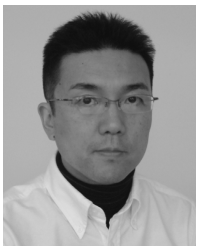

MIKIHIKO NISHIARA (Member, IEEE) received the B.Eng. degree in communication engineering from the Shibaura Institute of Technology, Tokyo, in 1992, and the M.Eng. and Ph.D. degrees in information systems from The University of Electro-Communications, Tokyo, in 1998 and 2001, respectively. From 2001 to 2007, he was a Research Assistant with the Graduate School of Information Systems, The University of Electro-Communications. Since 2007, he has been an Associate Professor with the Faculty of Engineering, Shinshu University. His research interests include information theory, including Shannon theory, data compression, and theoretical analysis of communication systems. He is a member of the IEICE.

OSAMU TAKYU (Member, IEEE) received the B.E. degree in electrical engineering from the Tokyo University of Science, Chiba, Japan, in 2002, and the M.E. and Ph.D. degrees in open and environmental systems from Keio University, Yokohama, Japan, in 2003 and 2006, respectively. From 2003 to 2007, he was a Research Associate with the Department of Information and Computer Science, Keio University. From 2004 to 2005, he was a Visiting Scholar with the School of Electrical and Information Engineering, The University of Sydney. From 2007 to 2011, he was an Assistant Professor with the Department of Electrical Engineering, Tokyo University of Science. He was an Assistant Professor, from 2011 to 2013, and has been an Associate Professor with the Department of Electrical and Electronic Engineering, Shinshu University, since 2013. His current research interests include wireless communication systems and distributed wireless communication technology. He was a recipient of the Young Researcher's Award of IEICE 2010 and the 2010 Active Research Award in Radio Communication Systems from the IEICE Technical Committee on RCS.

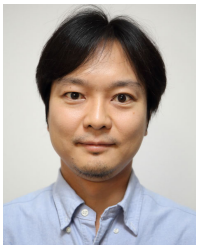

KOICHI ADACHI (Senior Member, IEEE) received the B.E., M.E., and Ph.D. degrees in engineering from Keio University, Japan, in 2005, 2007, and 2009 respectively.

From 2007 to 2010, he was a Japan Society for the Promotion of Science (JSPS) Research Fellow. He was a Visiting Researcher with the City University of Hong Kong, in April 2009, and a Visiting Research Fellow with the University of Kent, from June 2009 to August 2009. From May 2010 to May 2016, he was with the Institute for Infocomm Research, A*STAR, Singapore. He is currently an Associate Professor with The University of Electro-Communications, Japan. His research interests include cooperative communications and energy efficient communication technologies.

Dr. Adachi is a member of the IEICE. He was awarded the Excellent Editor Award from IEEE ComSoc MMTC, in 2013. He is a co-author of the WPMC2020 Best Student Paper Award. He served as the General Co-Chair for the 10th and 11th IEEE Vehicular Technology Society Asia Pacific Wireless Communications Symposium (APWCS), the Track Co-Chair for Transmission Technologies and Communication Theory of the 78th and 80th IEEE Vehicular Technology Conference, in 2013 and 2014, respectively, the Symposium Co-Chair for Communication Theory Symposium of IEEE Globecom 2018, the Tutorial Co-Chair for IEEE ICC 2019, and the Symposium Co-Chair for Wireless Communications Symposium of IEEE Globecom 2020. He was an Associate Editor of *IET Transactions on Communications*, from 2015 to 2017, IEEE Wireless Communications Letters, since 2016, IEEE Transactions on Vehicular Technology, from 2016 to 2018, IEEE Transactions on Green Communications and Networking, since 2016, and IEEE Open Journal of Vehicular Technology, since 2019. He was recognized as an Exemplary Reviewer from IEEE Wireless Communications Letters, in 2012, 2013, 2014, and 2015.